

The Challenge of Out-Of-Distribution Detection in Motor Imagery BCIs

Merlijn Quincent Mulder¹ , Matias Valdenegro-Toro¹ , Andreea Ioana Sburlea^{1*}  and Ivo Pascal de Jong^{1*} 

¹Department of Artificial Intelligence, University of Groningen
9747 AG Groningen, The Netherlands

E-mail: ivo.de.jong@rug.nl

Keywords: Out-Of-Distribution Detection, Uncertainty, Machine Learning, Brain Computer Interfaces, Motor Imagery

Abstract

Machine Learning classifiers used in Brain-Computer Interfaces make classifications based on the distribution of data they were trained on. When they need to make inferences on samples that fall outside of this distribution, they can only make blind guesses. Instead of allowing random guesses, these Out-of-Distribution (OOD) samples should be detected and rejected. We study OOD detection in Motor Imagery BCIs by training a model on some classes and observing whether unfamiliar classes can be detected based on increased uncertainty. We test seven different OOD detection techniques and one more method that has been claimed to boost the quality of OOD detection.

Our findings show that OOD detection for Brain-Computer Interfaces is more challenging than in other machine learning domains due to the high uncertainty inherent in classifying EEG signals. For many subjects, uncertainty for in-distribution classes can still be higher than for out-of-distribution classes. As a result, many OOD detection methods prove to be ineffective, though MC Dropout performed best. Additionally, we show that high in-distribution classification performance predicts high OOD detection performance, suggesting that improved accuracy can also lead to improved robustness.

Our research demonstrates a setup for studying how models deal with unfamiliar EEG data and evaluates methods that are robust to these unfamiliar inputs. OOD detection can improve the overall safety and reliability of BCIs.

*indicates shared last author.

1 Introduction

Machine Learning models make mistakes when they are tested on data that is dissimilar to what the models were trained on. Especially under *semantic shifts* – where a test sample belongs to a class that the model was never trained on – the model cannot possibly give a correct classification. Instead of giving an incorrect classification, a robust and reliable Machine Learning model should detect these samples that are *out-of-distribution* (OOD) with respect to the training data, and abstain from making a classification on them.

Machine Learning models used in Motor Imagery (MI) Brain-Computer Interfaces (BCIs) are also subject to this limitation. They are typically trained and evaluated with electroencephalography (EEG) data from two (e.g. left-hand, right-hand) to five (e.g. left, right, foot, tongue, rest) classes and are deployed with the assumption that all signals later must match one of these classes. In reality, it is very likely that users might perform actions not matching any of these classes at some point during usage [5]. Those OOD actions should be detected so that a device can abstain from making erroneous actions and instead prefer inaction.

The basic mechanism through which a Machine Learning model can detect OOD samples is through uncertainty. By indicating high uncertainty estimates for OOD samples, and low uncertainty estimates for in-distribution (ID) samples, the model can indicate whether a sample is likely to be OOD or not.

Achieving good separability between ID and OOD samples has only had limited attention in BCI research [5, 8], but in the broader Machine Learning literature, this topic has already attracted significant attention [7].

To achieve good OOD detection, various methods have been proposed. A unified discussion of these methods is presented in Yang *et al.* [32]. Mucsányi, Kirchhof, and Oh [18] highlighted that these different methods yield varying performance across tasks. Hence, there is a need for task-specific approaches when using uncertainty estimation methods for OOD detection. Notably, most methods have been developed for image classification problems, which risks that they cannot be applied to other domains with the same promise of performance. Particularly EEG is known to have large amounts of noise, which can lead to generally higher uncertainty estimates for the ID data, making OOD detection exceptionally difficult [8].

There has already been some interest in the task of OOD detection in EEG. Wong *et al.* [31] studied uncertainty and OOD detection in

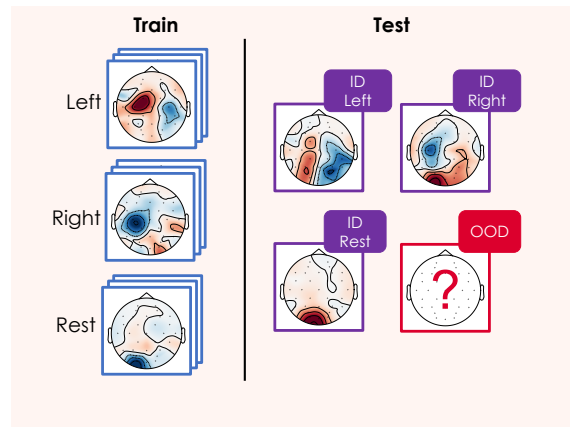


Figure 1: Concept of out-of-distribution detection. A model is trained on several known classes. It has to be able to recognize when unknown data does not belong to any of the known classes, while still classifying the known classes correctly.

epilepsy, and proposed a novel anomaly detection method using deep support vector data description and model uncertainty, showcasing an increase in the robustness of a model trained for seizure detection. However, they used OOD detection to identify patients that were dissimilar to the training data for which the model would not work well. Detecting samples within-subject that are OOD requires per-sample OOD detection. Wagh *et al.* [29] extensively studied uncertainty estimation under realistic EEG distribution shifts based on simulated instrumentation-related variabilities, but not brain-related variabilities, nor inference under unfamiliar classes.

Chetkin, Shishkin, and Kozyrskiy [5] previously studied OOD detection for Motor Imagery BCIs. They showed that OOD detection for BCI using Bayesian techniques, such as Markov Chain Monte Carlo samplers, is satisfactory only for some users. They argued that the use of effective prior distributions from computer vision is possibly not well-suited for BCI tasks, explaining the difference in OOD detection performance between the domains. Furthermore, classification and OOD detection are subject to the influences of the noise and variability in the signals between different distributions, making OOD detection more difficult for BCI tasks. Another factor is that patterns can differ between subjects, requiring within-subject training pipelines for good performance. The small, highly variable datasets further complicate OOD detection [21].

Chetkin, Shishkin, and Kozyrskiy [5] focused on Bayesian approaches for OOD detection in BCIs, and it is unclear whether the methods developed in other domains transfer effectively to BCI tasks. The current state of the art for

OOD detection in BCIs remains unknown, as do the factors that explain its performance.

In this study we establish the state of the art of OOD detection for BCIs, exploring a wide range of OOD detection methods for Convolutional Neural Networks (CNN) used in BCIs to identify which methods have the biggest impact on improving BCI robustness. We additionally investigate which factors have an impact on OOD detection performance, looking at in-distribution classification performance, specific classes that may be easier or harder to detect, and the activation strength of the penultimate layer in the neural network. Through this, we establish the current state-of-the-art, explain why OOD detection is exceptionally difficult in BCIs, and show how OOD detection may improve as on-task performance improves.

To this end, we benchmark seven OOD detection techniques spanning distance-based, Bayesian-based, and density-based approaches as defined in Section 2.2. We will use three different datasets (from [27, 22, 23]), available through Mother of all BCI Benchmarks (MOABB) [3]. As our CNN, we use EEGNeX, an optimised version of EEGNet that proved a reliable EEG signal decoding CNN-based architecture [4].

1.1 Contributions

By studying OOD detection in Motor Imagery BCIs, we make the following contributions:

- We demonstrate leave-one-class-out OOD detection as a challenging and useful experimental setup to simulate unfamiliar inputs that a BCI model will be exposed to in practice.
- We show that leave-one-class-out OOD detection is possible (but challenging) for BCIs with performance better than random guessing, in contrast to previous findings [8].
- We show that OOD detection performance correlates with classification performance. This means that OOD detection will get better as classification gets better.
- We find that methods that give good OOD detection in Computer Vision do not necessarily give good results for BCIs, because the amount of inherent uncertainty in BCIs is very high.
- We establish MC Dropout and Deep Ensembles as the state-of-the-art for BCI-OOD detection, and recommend these methods to improve BCI robustness.

Algorithm 1 LOCO-OOD experiment

```

1: hyperparameters  $\leftarrow$  tune(subjects[0])
2: for subject in subjects do
3:   for OOD-class in classes do
4:     train_data  $\leftarrow$  GET_TRAIN(subject)
                                      $\triangleright$  excludes OOD-class
5:     test_data  $\leftarrow$  GET_TEST(SUBJECT)
                                      $\triangleright$  includes OOD-class
6:     model  $\leftarrow$  EEGNEX()
7:     TRAIN(model, train_data)
8:     AUROC  $\leftarrow$  DETECT OOD(model,
                               test_data)
9:   end for
10: end for

```

1.2 Leave-one-class-out OOD Detection (LOCO-OOD)

We propose Leave One Class Out OOD Detection (LOCO-OOD) as an experimental paradigm to evaluate the performance of OOD detection models for BCIs.

LOCO-OOD trains models on a subset of classes available in the training dataset and evaluates it on all classes. That means there is one unseen class in the test dataset. A good OOD detection model should report higher uncertainty on the unseen class while still giving good predictions on the familiar classes. By applying a varying threshold on the estimated uncertainty, the unseen OOD class should be separated. How well the OOD class is separated can be measured with the Area Under the Receiver-Operator Characteristic curve (AUROC).

LOCO-OOD represents OOD samples that arise due to off-task behavior of the user. The model is trained on some classes, but when the user does something unfamiliar, the sample should be rejected. A model that performs well at LOCO-OOD is robust against these errors.

The procedure for LOCO-OOD experiments is specified in Algorithm 1.

2 Background

In this section we provide relevant background information. We provide a formal definition of OOD detection, introduce fundamental concepts of uncertainty, and briefly recap the essentials of Motor Imagery BCIs. Following this, we document existing OOD detection methods and provide a conceptual categorization.

2.1 Preliminaries

As defined by Yang et al. [32], a trustworthy recognition system is one that not only makes accurate predictions on known in-distribution (ID) data but can also reliably detect and reject

samples outside of this distribution. We define the ID as a joint distribution $P(X, Y)$, where $X \in \mathbb{R}^d$ is defined as the epoched input space and $Y \in \{y_1, \dots, y_k\}$ the label space. The training samples are drawn from this distribution through a calibration session. After training, when the model is ‘deployed’, it can encounter samples from a different distribution $P(X', Y')$. Then a sample $x', y' \sim P(X', Y')$ is OOD with respect to $P(X, Y)$ if the probability of the sample under the ID distribution $P(X=x', Y=y') \approx 0$. In our work, we create OOD samples with LOCO-OD. We set $Y' \in \{y_1, \dots, y_{k+1}\}$, so that for some y' it will be the case that $y' \notin \{y_1, \dots, y_k\}$, such that $P(Y=y') = 0$ which guarantees that $P(X=x', Y=y') = 0$.

The task for OOD detection is then to estimate $P(y' \in Y | X=x')$. This is a specific case of OOD detection where we define OOD samples as unfamiliar classes. OOD detection can be more broadly approached to consider unfamiliar examples of a known class, but defining OOD samples in those cases is more ambiguous. Effective OOD detection should identify inputs drawn from a distribution different from the training set without compromising ID classification performance.

Uncertainty Current OOD detection techniques rely on uncertainty estimators to distinguish between ID and OOD samples. This follows from the assumption that a model should output a prediction on a data point from an unknown distribution with low confidence. However, this is not always trivial [20]. Typically, studies separate uncertainty into two types [30]:

1. *Aleatoric uncertainty* is inherent to noise and ambiguity in the data, leading to low-confidence predictions. The aleatoric uncertainty is a consequence of the task not being perfectly ‘solvable’, leading to lower classification accuracy [12]. If aleatoric uncertainty is high in ID samples, it may interfere with OOD detection.
2. *Epistemic uncertainty* can be described as the lack of knowledge in the model. In the context of OOD samples belonging to different classes, this is a quantity that is high for a previously unseen input coming from a different distribution than the class distributions the model learned.

Correctly and truly disentangling the two types makes more reliable OOD detection for the definition of OOD previously mentioned. Currently, we do not have a good method for disentanglement [8]. A robust model will

account for both uncertainties. We will focus on detecting OOD samples using proven methods that do not always explicitly distinguish between the types.

MI-BCI paradigm In motor rehabilitation, BCIs are used to reintegrate the sensory-motor loop by directly accessing brain activity [2]. These motor interfaces translate neural signals into device commands, often relying on an endogenous task. Such tasks often require skills and experience to produce well-distinguishable brain patterns for accurate classification. The patterns are often recorded through EEG. Using differential amplification, waveforms are generated by comparing electrodes on the scalp, measuring voltage over time [14].

Typically, muscle activity is associated with Mu (8-12 Hz) and Beta (13-25 Hz) waves [14]. However, because EEG signals are generally weak, they are prone to artefacts that introduce noise before reaching the scalp. These noisy signals are later transformed into features encoding the user’s task from which control commands can be derived.

2.2 OOD Detection Approaches

We consider three distinct categories of OOD detection approaches, which are visualised in Figure 2. These categories are based on shared assumptions that various OOD detection methods make. Two different UQ methods per category will be used and compared in the experiment, next to softmax. Additionally, we include a general OOD detection optimisation technique.

2.2.1 Bayesian Based Traditionally, a Bayesian neural network is not only defined by its equations but also by its parameters. The latter can vary and therefore be encoded as a probability distribution estimated using Bayesian statistics. This differs from classical neural networks that use point-wise parameters. Hence, we can infer uncertainty by simulating how predictions would vary if we had a full Bayesian treatment of these parameters. We attempt this using MC Dropout and Deep Ensemble, as they are generally shown to perform well [18], and do not require altering the model structure and training process of the feature extractor. Although not strictly Bayesian, these methods approximate Bayesian inference by drawing samples from a variational posterior over the model parameters.

Monte Carlo (MC) Dropout Gal and Ghahramani [6] proposed to randomly remove neurons in the dropout layers during inference according to a predetermined dropout

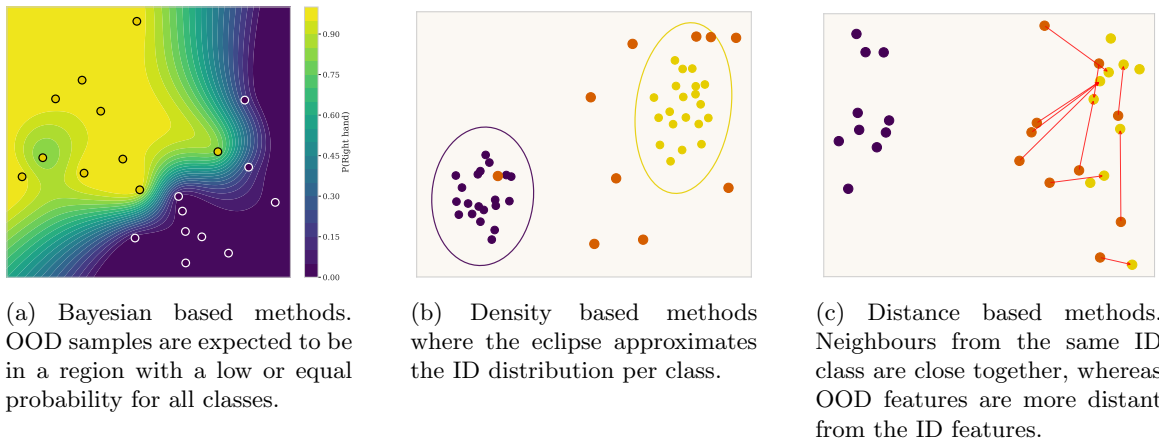


Figure 2: A visual explanation of three different OOD detection approaches. The data points belong to user nine of the BNCI2014 dataset. In this illustration **feet** is considered OOD on a model trained on the **right hand** and **left hand** classes.

probability. Through multiple forward passes with the same samples, you obtain a set of predictions corresponding to different configurations of the model. This approximates the posterior predictive distribution over the outputs. We measure the uncertainty using the entropy of the mean probabilities. This method can be applied to different architectures, such as CNNs incorporating dropout layers, where the dropout functionality is turned on during inference.

Deep Ensemble (DE) Lakshminarayanan, Pritzel, and Blundell [10] proposed aggregating inference results from multiple individually trained models with different weight initialisations and equal architecture. This can be done by setting different seeds for each individual model. Due to a difference in parameters, we effectively sample the parameter distribution of the model. The difference with MC Dropout is that we do not remove neurons in dropout layers during inference, but use multiple models.

2.2.2 Density Based Density-based methods estimate the ID distribution, quantifying the likelihood that an input is ID. This assumes a low likelihood for OOD samples to be part of this estimation. Generally, they consider a fixed distribution and are therefore parametric.

Energy Score Liu et al. [13] proposed the energy score as an alternative to softmax class probabilities. Theoretically, it aligns with the probability density of the inputs, being less susceptible to overconfidence and thereby improving distribution separation. Each input is mapped to a scalar using the energy function, which is lower for observed than unobserved

data.

A sample is classified as OOD if the energy score is larger than the score for an amount of ID samples under a predefined arbitrary threshold. Although not explicitly probabilistic, the energy score can be considered an implicit density method, as it can be extended into a probabilistic model using the Gibbs distribution [11], and relies on the assumption that higher density regions are more likely.

Deep Deterministic Uncertainty (DDU)

Mukhoti et al. [19] proposed to use Gaussian Discriminant Analysis (GDA) for epistemic uncertainty estimation and rely on the softmax predictive distribution for aleatoric uncertainty. In practice, they fit a Gaussian Mixture Model to the embeddings from the penultimate layer, which uses class-specific covariance matrices. A sample is considered OOD when the negative logarithmic density is lower than for ID samples. The authors argue that DDU can better separate uncertainties than other methods like DUQ with a high accuracy, especially on ambiguous datasets. As EEG data is often noisy and ambiguous, this can be an advantage.

2.2.3 Distance Based Distance-based UQ for OOD detection refers to a set of methods that estimate the uncertainty of a model’s prediction by measuring the distance between a given input and the ID training data in the feature space. These methods assume that samples relatively far away from the ID data are more likely to be OOD. Where density based methods assume a parametric distribution that may be incorrect, distance based methods only look at distances and are therefore not sensitive to incorrect assumptions.

Deterministic Uncertainty Quantification (DUQ) Proposed by Van Amersfoort et al. [28], DUQ computes the exponentiated distance between a feature embedding and centroids corresponding to each class. Using a similarity score, they quantify the model’s uncertainty, where the similarity is higher when a feature is closer to the class centroid in the feature space. When the similarity to all centroids is low and the distance is relatively long, a sample can be considered OOD. DUQ is composed of a (pre-trained) deep model used as a feature extractor and a radial basis function (RBF) network, using a class-dependent kernel, which can be trained separately. The latter takes the derived feature embedding as input. The kernel allows for feature insensitivity per class, which minimises the potential for feature collapse and leads to stable training.

The centroids are updated using an exponential moving average. The loss function for this method is calculated by taking the sum of the binary cross-entropy between each class’ kernel and a one-hot encoding of the label, effectively using a one vs. all loss function.

Deep k -Nearest Neighbour (d-KNN) Sun et al. [25] argued that simply deriving the k nearest neighbour distance from the feature embeddings performs poorly for OOD detection. Therefore, they proposed an optimisation computing a normalised feature embedding from the penultimate layer using L2 normalisation. This appeared crucial for good performance. For all training samples, the normalised feature embeddings are extracted and stored. When a new input sample is presented, its normalised feature embedding will be derived and compared to all stored embeddings using the Euclidean distance. From the sorted calculated distances, the k -th nearest neighbour is found. If this distance for a sample is relatively large compared to most ID samples, it can be considered OOD. This can be set with a threshold λ . d-KNN’s advantage over DUQ is that d-KNN is less computationally expensive, as it does not require training an additional model head with its own hyperparameters on top of the feature extractor.

2.2.4 OOD detection Optimisation In addition to evaluating OOD detection methods, this study investigates Rectified Activations (ReAct) as a general OOD optimisation technique to enhance OOD detection performance. This technique is designed to be used in conjunction with other approaches and can be applied across all OOD detection methods.

Rectified Activations (ReAct) OOD inputs can cause activation patterns in hidden layers of the Neural Network that significantly deviate from those produced by ID data, as shown in image classification tasks [24]. This results in larger variations across activations biased towards having high values, leading to model overconfidence. By applying an element-wise function to the penultimate layer, you can truncate activations above a limit c to limit the effect of noise. This variable is set based on the p -th percentile of activations estimated on ID data. Combining this technique with d-KNN or energy-based OOD proved better performance [24]. This is especially the case when OOD samples’ activations have a large variance and are positively skewed.

3 Methods

This paper performs a LOCO-ODD experiment, as introduced in Section 1.2, for which we will present the implementation below. We then present our feature extractor, the three datasets used in this paper, and various OOD detection methods divided into three categories, along with two OOD optimisation techniques. Lastly, we present multiple analyses that we perform on the data gathered from the experiment.

3.1 Experiment implementation

We implement a within-subject LOCO-ODD experiment. We rotate the classes to be defined as OOD to simulate real-life OOD detection. The model is not trained on the data of the OOD class. From the ID dataset, 10% is used for validation and 15% is used for testing. This was achieved using a stratified split. The total test set has a 1:1 ID-ODD ratio. The remaining 75% of the ID dataset is used to train the feature extractor.

We run MC-Dropout with 50 forward passes and use 5 models in the Deep Ensemble. The distance-based methods require hyperparameter tuning on the first user in the dataset. Therefore, the data of the first user will then be excluded during testing. The hyperparameter is dependent on the OOD class, as this provides a different class combination in the training data. For d-KNN, we select the k producing the largest Area Under the Receiver Operating Characteristic Curve (AUROC), testing the separability of ID and OOD. We restrict the maximum k to the mean number of training data points per class. As DUQ has multiple hyperparameters that are dependent on each other, we use the Optuna hyperparameter optimisation framework [1] with the search space as defined in Table D2. The found optimal hyperparameters are available in Table D1. Furthermore, we train DUQ as a separate

	BNCI2014	Schirrmeister2017	Stieger2021
#Subjects	9	12	62
#Channels	22	128	64
#Classes	4	4	4
#Trials/class	144	120	450
Trial length	4s	4s	3s
Frequency	250Hz	500Hz	1000Hz

Table 1: Summary of the datasets.

head with a learnable length scale per class on top of our frozen feature extractor. This differs from [28], which jointly trains the DUQ head and the feature extractor.

We apply z-score normalisation to all EEG data after the split and before further usage.

3.2 Feature extraction

As the feature extractor for all experiments, we use a PyTorch implementation of EEGNeX [4], a compact deep learning model designed for EEG signal classification. It consists of 8 convolutional blocks optimised for spatiotemporal feature learning across EEG channels and time windows. Additionally, we extend the model with spectral normalisation applied to the penultimate convolutional linear layer for better class separation in latent space, which is essential for OOD methods like DDU [19]. Lastly, we train the model on batches of size 32 using a cross-entropy (CE) loss and an Adam optimiser [9] with a learning rate of $1 \cdot 10^{-3}$ on all datasets. We use early stopping with a patience of 20 and half the learning rate with a patience of 5 to prevent overfitting, with a maximum of 200 epochs. The best-performing model from the training cycle will be used as the feature extractor in the experiments.

3.3 Datasets

Within this study, we use the three different MI-BCI and Motor Execution (ME) BCI datasets from MOABB [3]. The datasets complement each other as they differ in their technical setup, such as the number of channels, the sampling frequency, and the number of data points per user, as seen in Table 1. All datasets contain four classes corresponding to different movements, as seen in Table 2. We use all the data after applying a bandpass filter from 7.0 to 35.0 Hz, following the default configuration in MOABB. No ICA or artifact rejection is applied. Unless specified, we do not discard any data throughout the experiments.

BNCI2014 This is dataset IIA from BCI competition IV [27]. The data is from a cue-based BCI paradigm corresponding to different MI tasks. Participants were seated in a comfortable chair watching a screen on which an

Class	Movement
<i>BNCI2014</i>	
Left hand	Movement left hand
Right hand	Movement right hand
Both feet	Movement feet
Tongue	Movement tongue
<i>Schirrmeister2017</i>	
Left hand	Sequential finger tapping
Right hand	Sequential finger tapping
Feet	Clench toes
Rest	Voluntary rest
<i>Stieger2021</i>	
Left hand	Left hand open and close
Right hand	Right hand open and close
Both hands	Both hands open and close
Rest	Voluntary rest

Table 2: Classes and movements in the datasets. The Schirrmeister2017 dataset contains executed movements; the other datasets contain imagined movements.

arrow was presented corresponding to a class, prompting a participant to imagine the movement.

Schirrmeister2017 This dataset results from an experiment where subjects perform a repetitive movement requiring little proximal muscular activity [22]. The movements were executed depending on the direction of an arrow. The experiment was originally done in a lab setting with 128 channels, out of which 44 were used for the motor cortex.

Stieger2021 Originally, this dataset results from a study investigating how individuals learn to control sensorimotor rhythm BCIs [23]. In total, 33 participants went through an eight-week mindfulness program, and 29 participants were assigned the control condition. Both groups received BCI training before the experimental data were obtained. During the experiment, participants had to move a cursor on a screen using hand movements. The data from both groups are used in this experiment. Some channels were previously marked as bad by MOABB. In this study, we only use the intersection of the channels not marked as bad per participant across sessions.

3.4 Analyses

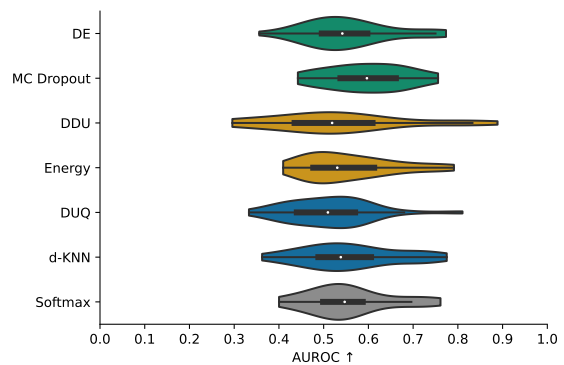
We perform multiple analyses on the results of the predefined experiment. These include comparing the OOD detection methods, OOD optimization techniques, and the differences between OOD classes.

3.4.1 OOD approach comparison We perform the experiment on all three predefined datasets. For each dataset, we calculate the AUROC per OOD detection method for all participants and possible OOD classes. To study the relation between the AUROC scores and the model and datasets, we use a linear mixed-effects model. Within this model, we treat the participants as a random effect, as multiple data points belong to the same participant. The BCNI2014 dataset and Softmax will be the baseline to which the interactions will be compared. Furthermore, we will perform pairwise comparisons between the UQ methods using the estimated marginal means averaged over the datasets and a z-test with Holm correction. As a measure of central tendency, we will report the median (Mdn) due to differing distributions of AUROC per result that do not always follow a normal distribution.

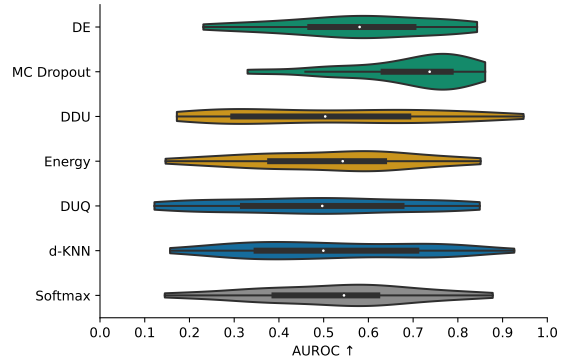
3.4.2 Class dependent OOD As OOD performance might differ depending on the class selected as OOD with differing EEG features, we separate the AUROC values based on the OOD class and test for significance using a Kruskal-Wallis test.

3.4.3 Classification vs OOD detection performance As better-performing models are more proficient at correctly classifying samples, it is likely that they can separate features in the feature space better. This has the potential to support the OOD detection methods in distinguishing OOD from ID. Therefore, we test whether there is a correlation between the model’s on-task performance and the OOD detection performance per detection approach using Spearman’s Rank Correlation. As Deep Ensemble and DUQ involve additional trainable parameters, we evaluate the on-task performance of those additional parameters. As there is no meaningful difference on MI-BCI between MC Dropout classification and inference with a full model [15], we assume the same on-task performance. We perform this analysis on both on-task AUROC gathered for models trained on three and two ID classes.

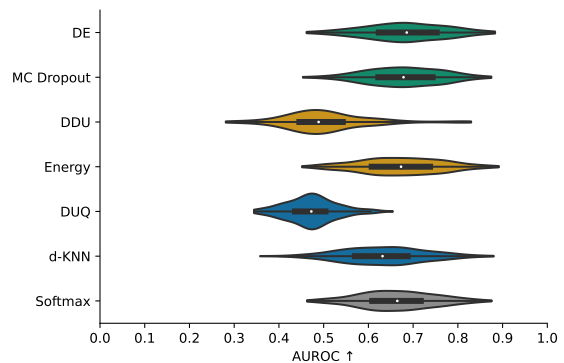
3.4.4 OOD optimization We determine whether ReAct[24] can boost the ability of the OOD detection approaches to distinguish OOD from ID. We will keep the same pipeline as for the previous experiments. We will add ReAct to the feature extractors’ outputs before feeding this to the OOD detection methods and test this on all datasets. We will determine significance using a Wilcoxon signed-rank test.



(a) BCNI2014 dataset.



(b) Schirrmeister2017 dataset.



(c) Stieger2021 dataset.

Figure 3: Performance of OOD detection methods across three datasets. Colours indicate the following UQ categories: Bayesian, Density, Distance, Baseline.

4 Results

We will show the differences in OOD-detection performance across both the methods and the datasets as the main analysis. Following this, we investigate class differences, the correlation between on-task performance and OOD detection, and optimization methods as further analysis.

4.1 OOD approach comparison

Figure 3 shows violin plots of the OOD detection performances over different methods and datasets, with medians and interquartile ranges reported in Table 3. We support this

analysis with a linear mixed effects model (LMM) to explore the differences between the OOD detection methods and the datasets, with Softmax serving as our baseline and the BNCI2014 dataset that converged to an intercept AUROC of 0.554.

MC Dropout receives the highest AUROC scores for OOD detection with MI-BCI data on both the BNCI2014 ($Mdn=0.597$) and Schirrneister2017 ($Mdn=0.737$) datasets. This is evident in Figures 3a and 3b.

The latter demonstrates an increase in spread for all methods. However, we cannot conclude that performance on the Schirrneister2017 dataset is significantly worse ($p=0.404$, $Coef.= -0.027$). Simultaneously, we do observe that MC Dropout performs significantly better on this dataset ($p=5.816 \cdot 10^{-5}$, $Coef.=0.123$).

Furthermore, on the Stieger2021 dataset, DDU ($p=1.283 \cdot 10^{-7}$, $Coef.= -0.135$) and DUQ ($p=4.220 \cdot 10^{-9}$, $Coef.= -0.150$) show significantly worse performance compared to the other methods as seen in Figure 3c.

Contrastingly, in general, the OOD detection methods perform better on the Stieger2021 dataset ($p=5.669 \cdot 10^{-5}$, $Coef.=0.109$). The full LMM results can be seen in Table C1.

When performing a z-test using estimated marginal means, we observe that MC dropout outperforms all other methods ($p < 0.001$). DUQ and DDU perform similarly ($p = 0.107$, Estimated difference = 0.025), but significantly worse than the remaining methods ($p < 0.001$). We do not find a significant difference between the other approaches. The full pairwise comparison is available in Table C2.

When models are trained on fewer classes, this can also affect OOD detection performance. This is explored in Appendix B.

4.2 Class-dependent OOD detection

When comparing AUROC scores across different OOD classes within each dataset, we observe clear class-dependent differences in OOD detectability that are statistically significant for all datasets except BNCI2014 ($p = 5.510 \cdot 10^{-2}$, $H = 7.598$), as shown in Figure 4.

In the Schirrneister2017 dataset ($p = 4.498 \cdot 10^{-3}$, $H = 13.065$), we observe that the Rest class is easier to detect as OOD than the Left hand class ($p = 1.930 \cdot 10^{-4}$) as shown in Figure 4b. However, this class-dependent behavior is not consistent across all detection methods. For instance, hand movement classes achieve higher AUROC scores when using MC Dropout, whereas the opposite trend is observed when using DDU.

For the Stieger2021 dataset, we again find significant class-dependent differences in OOD

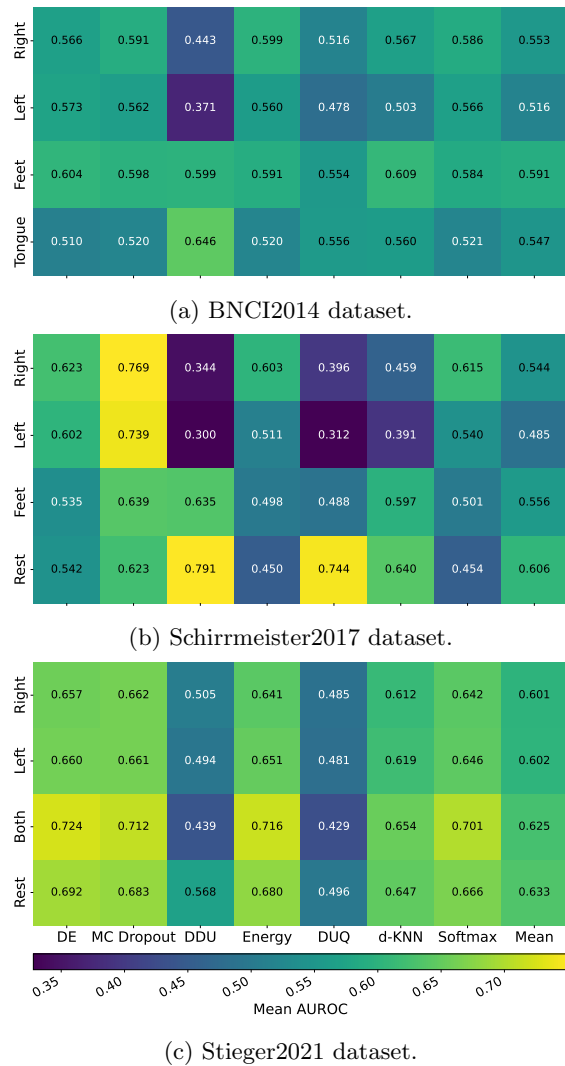


Figure 4: Performance of OOD detection for different classes plotted against the different UQ methods. “Left”, “Right” and “Both” refer to hand movements. Whilst the performance for the Left and Right hand classes stays relatively similar, we find a significant increase in AUROC for the Both hands and Feet classes.

detection performance ($p = 3.878 \cdot 10^{-6}$, $H = 27.864$). The Rest class is significantly easier to detect as OOD than both the Right hand ($p = 2.670 \cdot 10^{-4}$) and Left hand ($p = 1.197 \cdot 10^{-3}$) classes. As shown in Figure 4c, a similar effect is observed for the Both hands class, which is easier to detect as OOD than the Right ($p = 1.248 \cdot 10^{-3}$) and Left hand ($p = 4.916 \cdot 10^{-3}$) classes.

4.3 Classification vs OOD detection performance

We examine the relation between classification performance and OOD detection performance. We see a non-linear relation in Figure 5, where the OOD detection performance increases with the classification performance for the Bayesian

Method	Median	IQR	p_{ReAct}	$p_{correlation}$	$\rho_{correlation}$	On-Task AUROC
<i>BNCI2014</i>						
Deep Ensemble	0.542	0.102	0.026	$3.877 \cdot 10^{-13}$	0.586	0.852
MC Dropout	0.597	0.124	0.145	$8.857 \cdot 10^{-12}$	0.557	0.837
DDU	0.519	0.174	0.945	0.558	0.052	0.837
Energy	0.530	0.136	0.537	$4.400 \cdot 10^{-12}$	0.563	0.837
DUQ	0.509	0.130	0.873	.037	0.185	0.772
d-KNN	0.538	0.118	0.898	$1.658 \cdot 10^{-6}$	0.409	0.837
Softmax	0.547	0.089	0.737	$4.863 \cdot 10^{-13}$	0.584	0.837
<i>Schürmeister2017</i>						
Deep Ensemble	0.580	0.231	0.639	$1.448 \cdot 10^{-8}$	0.380	0.961
MC Dropout	0.737	0.150	0.171	$1.526 \cdot 10^{-10}$	0.425	0.958
DDU	0.504	0.391	0.698	0.271	0.077	0.958
Energy	0.543	0.255	0.013	$1.757 \cdot 10^{-7}$	0.353	0.958
DUQ	0.499	0.354	0.764	0.463	0.051	0.816
d-KNN	0.499	0.357	$3.000 \cdot 10^{-5}$	$7.349 \cdot 10^{-4}$	0.232	0.958
Softmax	0.545	0.230	$8.729 \cdot 10^{-3}$	$4.842 \cdot 10^{-8}$	0.367	0.958
<i>Stieger2021</i>						
Deep Ensemble	0.686	0.129	1.000	$4.296 \cdot 10^{-174}$	0.746	0.923
MC Dropout	0.679	0.121	1.000	$3.136 \cdot 10^{-238}$	0.830	0.912
DDU	0.489	0.100	$1.030 \cdot 10^{-12}$	0.099	-0.053	0.912
Energy	0.673	0.130	1.000	$1.358 \cdot 10^{-180}$	0.755	0.912
DUQ	0.472	0.070	0.970	0.919	0.919	0.003
d-KNN	0.632	0.118	1.000	$8.357 \cdot 10^{-104}$	0.618	0.912
Softmax	0.665	0.109	1.000	$1.894 \cdot 10^{-193}$	0.771	0.912

Table 3: The OOD detection performance (*Median*) and spread (*IQR*) measured through AUROC per method resulting from the OOD approach comparison. Using a Wilcoxon signed-rank test (p_{ReAct}), we find that ReAct does not improve OOD optimisation. Using Spearman’s rank correlation test ($p_{correlation}$, $\rho_{correlation}$) between classification performance and OOD detection performance without ReAct, we find a non-linear correlation for multiple results. Bonferroni corrected $\alpha = 2.381 \cdot 10^{-3}$. On-Task AUROC refers to the average classification performance on ID data for a model trained on three ID classes. Several OOD detection methods do not affect ID classification and therefore have the same on-task performance.

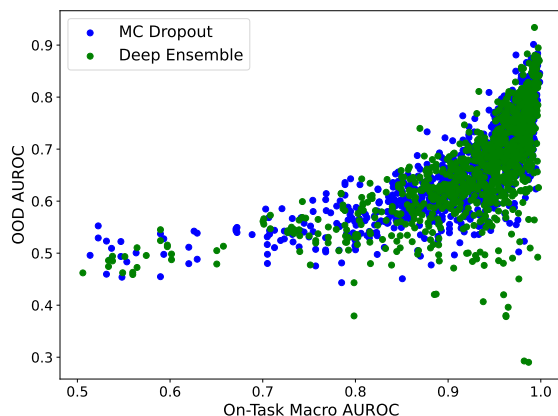


Figure 5: OOD detection vs on-task classification performance on Bayesian approaches showing a non-linear correlation on the Stieger2021 dataset.

methods when performing the experiment with the Stieger2021 dataset, with further results given in Appendix A. Table 3, shows that we did not detect this relation for DDU and DUQ. We can conclude for all other methods on all

tested datasets that it is easier to detect an OOD sample with a high on-task performance.

4.4 OOD optimisation

OOD detection methods can benefit from ReAct as an optimization. We analyse whether ReAct is effective for OOD detection with MI-BCI as well.

4.4.1 ReAct Figure 6 illustrates how ReAct affects performance when activations are clamped on the 90th percentile of the ID train data. For DDU ($1.030 \cdot 10^{-12}$), we observe that the peak lies slightly after 0.0, indicating a higher probability of a small improvement, which is statistically significant on the Stieger2021 dataset. Accounting for multiple comparisons with Bonferroni correction in Table 3, ReAct does not show a significant improvement on the other models and datasets.

5 Discussion

Well-performing OOD detection in MI-BCI have the potential to make systems more robust when

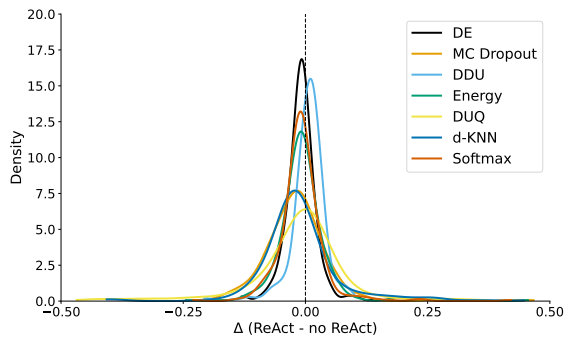


Figure 6: Difference in AUROC when using ReAct aggregated over all datasets. Smoothing was done using KDE. The dotted line indicates no difference

encountering data outside of the ID distribution. As OOD detection is an underexplored topic in Brain-Computer Interfaces, we aimed to answer which OOD detection method is most effective in MI datasets using CNN-based architectures and the possible reasons for its performance. In the following sections, we will explore the findings of our experiment.

5.1 Findings

We conclude that MC Dropout is the most reliable OOD detection method for Motor Imagery BCIs, followed by Deep Ensembles. However, the performance differs per dataset. Deep Ensembles and MC Dropout are both approximations of Bayesian Neural Networks, suggesting that previous works on Bayesian Neural Networks in BCIs [16, 17, 26] are also promising for OOD detection.

Moreover, we found that some OOD classes are easier to detect than others. We found a non-linear correlation between the model performance and the OOD detection performance, especially for the Bayesian and density-based methods.

Sun, Guo, and Li [24] argued that OOD samples can have higher activations than ID samples, leading to overconfidence, and hence, activations should be clamped. However, we find that, on average, ReAct does not improve the OOD detection methods when working with MI and ME BCI data. Sometimes, not clamping the activations can lead to better OOD detection.

Within the experiment, we noticed that methods in some runs performed worse than random. This means the UQ method is assigning higher uncertainty to ID samples, while that should be the case for OOD samples.

5.2 Interpretations and limitations

Domain differences. Benchmarking studies such as Mucsányi, Kirchhof, and Oh [18] performed with image data not only show better

OOD detection, but also a smaller variance between models and runs than we find. BCI data is more difficult to model due to noisy signals and uncertainties in the data. Given the differences in data, findings from computer vision do not guarantee translation into BCI applications, as illustrated by our findings.

Dataset differences. We found a difference in the difficulty of OOD detection and the optimal OOD detection method between the datasets.

We notice that the OOD detection results are lower on the Schirmer2017 dataset, where the data was recorded with 128 channels. The results are similar for datasets with 22 and 64 channels. As only 44 channels out of the 128 were used for the motor cortex, the measuring setup could have introduced unnecessary and potentially noisy information. This can make it more difficult for the model to extract the relevant details from the signal needed to detect OOD.

Notably, the Stieger2021 dataset contained more samples per participant per class, providing a better approximation of the distribution of possible ID samples. As a machine learning model can improve from being trained on more data, this can lead to a better model and possibly more reliable OOD detection.

Class dependent OOD. We show that the *Both hands* and *Rest* classes are easier to detect as OOD across datasets, although this can differ per UQ method. For all datasets, the results for the left and right hands are relatively similar within the dataset. This can be explained by the signals being a roughly symmetrical reflection of each other at the other side of the scalp. Both hands likely have double the activations compared to using one hand, and the *Rest* class has none or little, as no muscle is actively stimulated.

Classification performance vs. OOD detection. We found that classification performance is predictive of OOD detection performance with the exception of DDU and DUQ. This is most apparent in the results using the Stieger2021 dataset, as we produced more data points with this dataset. This relationship concludes that if the model has good on-task performance, then OOD samples will be easier to detect.

ReAct We found that ReAct does not lead to better OOD detection for most UQ methods. ReAct works by clamping activations when the activations for OOD samples are higher than for

ID samples. We noticed that often the activations for ID samples were higher than for OOD samples, and therefore ReAct showed no improvement to the quality of OOD detection.

5.3 Future Research

We found a correlation between model performance and OOD detection; a better-performing model is beneficial for OOD detection. If we find a better model that separates the signals better, it is likely that OOD samples will become easier to detect. Future work may explore how training improves not only the accuracy of the model over sessions, but also the OOD detection ability.

Our experiments rely on a LOCO-OOD task. This means we test the OOD detection ability methods on classes unknown to the model. While this is one of the challenges for a robust BCI system, there are other OOD applications for BCIs. For example, EEG signals deal with artefacts, which could be detected using OOD methods as well.

Hence, we need to define what we require from OOD detection for MI-BCI. Then we can establish if OOD detection methods work for different applications and predict which method works best for specific problems.

5.4 Conclusion

In summary, we found several UQ methods that perform well on OOD detection. We recommend MC-Dropout and Deep Ensembles for their good on-task performance and OOD detection performance.

Some OOD classes are easier to detect than others, and OOD optimisation techniques such as ReAct are not guaranteed to work with MI-BCIs. However, we conclude that the problem of OOD detection for BCIs remains unsolved, as performance differs on datasets, and the OOD detection methods do not always perform better than random. As the applications also differ from other domains, we need a BCI-specific definition and possibly a recommendation to train participants before BCI use to improve the detection of OOD signals.

Data availability

The codebase for this study is available at the following GitHub repository:
<https://github.com/MerlijnQ/OOD-BCI>

References

- [1] Takuya Akiba et al. “Optuna: A Next-generation Hyperparameter Optimization Framework”. In: *Proceedings of the 25th ACM SIGKDD International Conference on Knowledge Discovery and Data Mining*. 2019.
- [2] Luz Maria Alonso-Valerdi, Ricardo Antonio Salido-Ruiz, and Ricardo A. Ramirez-Mendoza. “Motor imagery based brain–computer interfaces: An emerging technology to rehabilitate motor deficits”. In: *Neuropsychologia* 79 (2015), pp. 354–363. DOI: <https://doi.org/10.1016/j.neuropsychologia.2015.09.012>.
- [3] Bruno Aristimunha et al. *Mother of all BCI Benchmarks*. Version 1.0.0. 2023. DOI: <https://doi.org/10.5281/zenodo.10034223>.
- [4] Xia Chen et al. “Toward reliable signals decoding for electroencephalogram: A benchmark study to EEGNeX”. In: *Biomedical Signal Processing and Control* 87 (2024), p. 105475. DOI: <https://doi.org/10.1016/j.bspc.2023.105475>.
- [5] Egor I. Chetkin, Sergei L. Shishkin, and Bogdan L. Kozyrskiy. “Bayesian Opportunities for Brain–Computer Interfaces: Enhancement of the Existing Classification Algorithms and Out-of-Domain Detection”. In: *Algorithms* 16.9 (2023). DOI: <https://doi.org/10.3390/a16090429>.
- [6] Yarin Gal and Zoubin Ghahramani. “Dropout as a Bayesian Approximation: Representing Model Uncertainty in Deep Learning”. In: *Proceedings of The 33rd International Conference on Machine Learning*. Vol. 48. PMLR, 2016, pp. 1050–1059. URL: <https://proceedings.mlr.press/v48/gal16.html>.
- [7] Navid Ghassemi and Ehsan Fazl-Ersi. “A Comprehensive Review of Trends, Applications and Challenges In Out-of-Distribution Detection”. 2022. URL: <https://arxiv.org/abs/2209.12935>.
- [8] Ivo Pascal de Jong, Andreea Ioana Sburlea, and Matias Valdenegro-Toro. “How disentangled are your classification uncertainties?” 2024. DOI: <https://doi.org/10.48550/arXiv.2408.12175>.
- [9] Diederik P. Kingma and Jimmy Ba. “Adam: A Method for Stochastic Optimization”. 2017. URL: <https://arxiv.org/abs/1412.6980>.
- [10] Balaji Lakshminarayanan, Alexander Pritzel, and Charles Blundell. “Simple and Scalable Predictive Uncertainty Estimation using Deep

- Ensembles”. In: *Advances in Neural Information Processing Systems*. Vol. 30. 2017. URL: https://proceedings.neurips.cc/paper_files/paper/2017/file/9ef2ed4b7fd2c810847ffa5fa85bce38-Paper.pdf.
- [11] Yann LeCun et al. “A tutorial on energy-based learning”. In: *Predicting structured data 1.0* (2006).
- [12] Hao Li et al. “Prototype-based Aleatoric Uncertainty Quantification for Cross-modal Retrieval”. In: *Advances in Neural Information Processing Systems*. Vol. 36. 2023, pp. 24564–24585. URL: https://proceedings.neurips.cc/paper_files/paper/2023/file/4d893f766ab60e5337659b9e71883af4-Paper-Conference.pdf.
- [13] Weitang Liu et al. “Energy-based Out-of-distribution Detection”. In: *Advances in Neural Information Processing Systems*. Vol. 33. 2020, pp. 21464–21475. URL: https://proceedings.neurips.cc/paper_files/paper/2020/file/f5496252609c43eb8a3d147ab9b9c006-Paper.pdf.
- [14] Erik K. St Louis et al. “An Orderly Approach to EEG Analysis”. en. In: *Electroencephalography (EEG): An Introductory Text and Atlas of Normal and Abnormal Findings in Adults, Children, and Infants [Internet]*. American Epilepsy Society, 2016. URL: <https://www.ncbi.nlm.nih.gov/books/NBK390342/>.
- [15] Prithviraj Manivannan et al. “Uncertainty Quantification for cross-subject Motor Imagery classification”. 2024. URL: <https://arxiv.org/abs/2403.09228>.
- [16] Daily Milanés-Hermosilla et al. “Monte Carlo Dropout for Uncertainty Estimation and Motor Imagery Classification”. In: *Sensors* 21.21 (2021). DOI: [10.3390/s21217241](https://doi.org/10.3390/s21217241).
- [17] Daily Milanés-Hermosilla et al. “Robust Motor Imagery Tasks Classification Approach Using Bayesian Neural Network”. In: *Sensors* 23.2 (2023). DOI: [10.3390/s23020703](https://doi.org/10.3390/s23020703).
- [18] Bálint Mucsányi, Michael Kirchhof, and Seong Joon Oh. “Benchmarking Uncertainty Disentanglement: Specialized Uncertainties for Specialized Tasks”. In: *Advances in Neural Information Processing Systems*. Vol. 37. 2024, pp. 50972–51038. URL: https://proceedings.neurips.cc/paper_files/paper/2024/file/5afa9cb1e917b898ad418216dc726fbd-Paper-Datasets_and_Benchmarks_Track.pdf.
- [19] Jishnu Mukhoti et al. “Deep Deterministic Uncertainty: A New Simple Baseline”. en. In: *2023 IEEE/CVF Conference on Computer Vision and Pattern Recognition (CVPR)*. IEEE, 2023, pp. 24384–24394. DOI: <https://doi.org/10.1109/CVPR52729.2023.02336>.
- [20] Anh Nguyen, Jason Yosinski, and Jeff Clune. “Deep Neural Networks Are Easily Fooled: High Confidence Predictions for Unrecognizable Images”. In: *Proceedings of the IEEE Conference on Computer Vision and Pattern Recognition (CVPR)*. 2015.
- [21] Jaime A Riascos, Marta Molinas, and Fabien Lotte. “Machine Learning Methods for BCI: challenges, pitfalls and promises”. en. In: *ESANN 2024 proceedings*. 2024, pp. 555–564. DOI: <https://doi.org/10.14428/esann/2024.ES2024-4>.
- [22] Robin Tibor Schirrmeister et al. “Deep learning with convolutional neural networks for EEG decoding and visualization”. en. In: *Human Brain Mapping* 38.11 (2017), pp. 5391–5420. DOI: <https://doi.org/10.1002/hbm.23730>.
- [23] J R Stieger, S A Engel, and B He. “Continuous sensorimotor rhythm based brain computer interface learning in a large population”. In: *Scientific Data* 8.1 (2021), p. 98. DOI: <https://doi.org/10.1038/s41597-021-00883-1>.
- [24] Yiyoun Sun, Chuan Guo, and Yixuan Li. “ReAct: Out-of-distribution Detection With Rectified Activations”. In: *Advances in Neural Information Processing Systems*. Vol. 34. 2021, pp. 144–157. URL: https://proceedings.neurips.cc/paper_files/paper/2021/file/01894d6f048493d2cacde3c579c315a3-Paper.pdf.
- [25] Yiyoun Sun et al. “Out-of-Distribution Detection with Deep Nearest Neighbors”. In: *Proceedings of the 39th International Conference on Machine Learning*. Vol. 162. PMLR, 2022, pp. 20827–20840. URL: <https://proceedings.mlr.press/v162/sun22d.html>.
- [26] Joris Suurmeijer et al. “Uncertainty Quantification for Motor Imagery BCI–Machine Learning vs. Deep Learning”. In: *2025 IEEE 35th International Workshop on Machine*

- Learning for Signal Processing (MLSP)*.
IEEE. 2025, pp. 1–6.
- [27] Michael Tangermann et al. “Review of the BCI competition IV”. In: *Frontiers in neuroscience* 6 (2012), p. 55. DOI: <https://doi.org/10.3389/fnins.2012.00055>.
- [28] Joost Van Amersfoort et al. “Uncertainty Estimation Using a Single Deep Deterministic Neural Network”. In: *Proceedings of the 37th International Conference on Machine Learning*. Vol. 119. PMLR, 2020, pp. 9690–9700. URL: <https://proceedings.mlr.press/v119/van-amersfoort20a.html>.
- [29] Neeraj Wagh et al. “Evaluating Latent Space Robustness and Uncertainty of EEG-ML Models under Realistic Distribution Shifts”. In: *Advances in Neural Information Processing Systems*. Vol. 35. 2022, pp. 21142–21156. URL: https://proceedings.neurips.cc/paper_files/paper/2022/file/8511d06d5590f4bda24d42087802cc81-Paper-Conference.pdf.
- [30] Tianyang Wang et al. “From Aleatoric to Epistemic: Exploring Uncertainty Quantification Techniques in Artificial Intelligence”. 2025. DOI: <https://doi.org/10.48550/arXiv.2501.03282>.
- [31] Sheng Wong et al. “Estimating Patient-Level Uncertainty in Seizure Detection Using Group-Specific Out-of-Distribution Detection Technique”. en. In: *Sensors* 23.20 (2023), p. 8375. DOI: <https://doi.org/10.3390/s23208375>.
- [32] Jingkang Yang et al. “Generalized Out-of-Distribution Detection: A Survey”. en. In: *International Journal of Computer Vision* 132.12 (2024), pp. 5635–5662. DOI: <https://doi.org/10.1007/s11263-024-02117-4>.

A Classification vs OOD detection performance

Figure A1 demonstrates the non-linear correlation between on-task performance and OOD detectability per dataset and UQ category. This correlation indicates that on-task performance is predictive of OOD detection performance with the exception of DDU and DUQ.

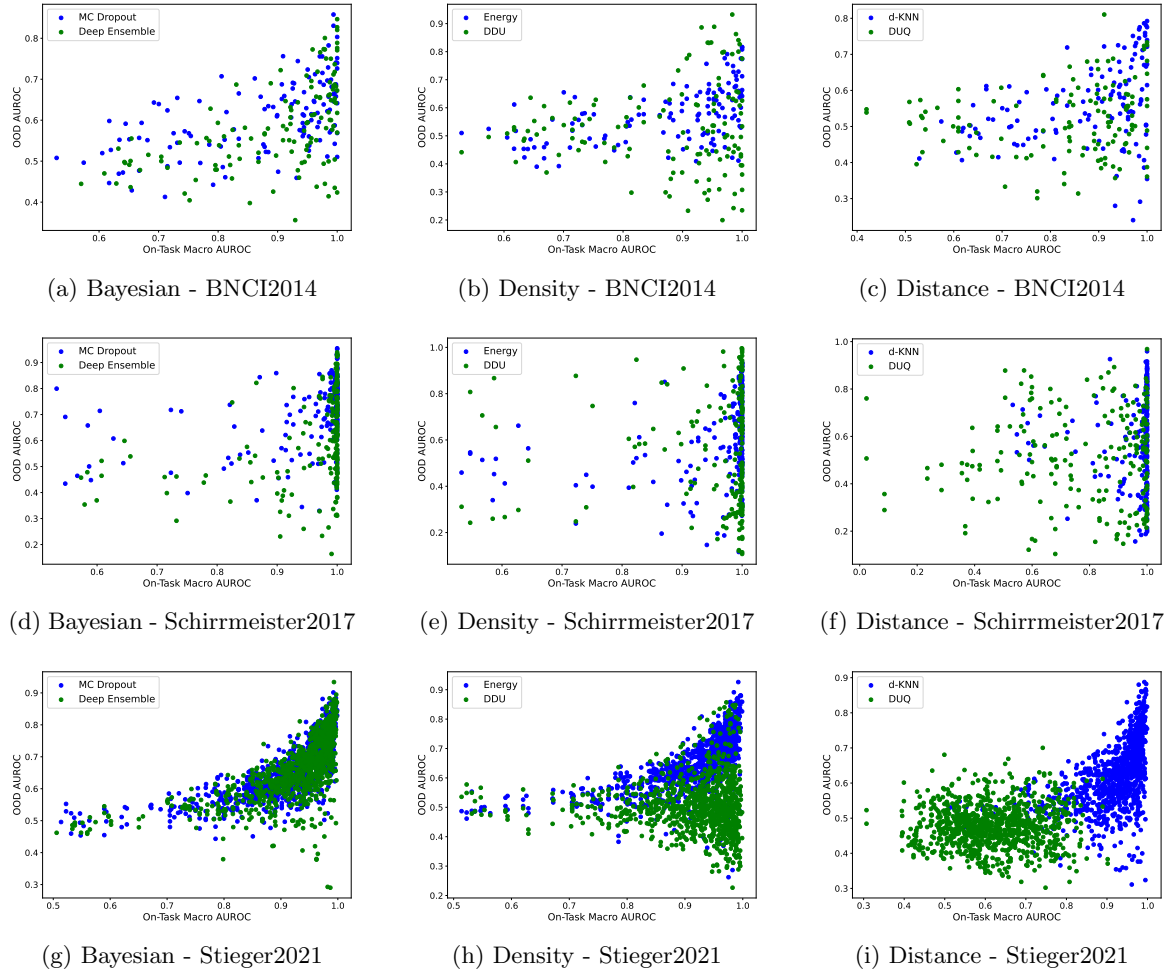


Figure A1: OOD detection vs on-task classification performance for models trained on two and three ID classes.

B Difference in number of ID classes

Figure B1b indicates that OOD detection may be easier when the model is trained on fewer classes. However, as shown in Table B1, this effect is statistically significant only for the energy score on the Schirrmeister2017 dataset. This pattern is inconsistent with the results for the Stieger2021 dataset (Figure B1c). In that case, a significant difference is only observed for DE, energy score, and MC dropout, which perform better when the model is trained on three ID classes. For the BNCI2014 dataset (Figure B1a) we do not observe statistically significant differences.

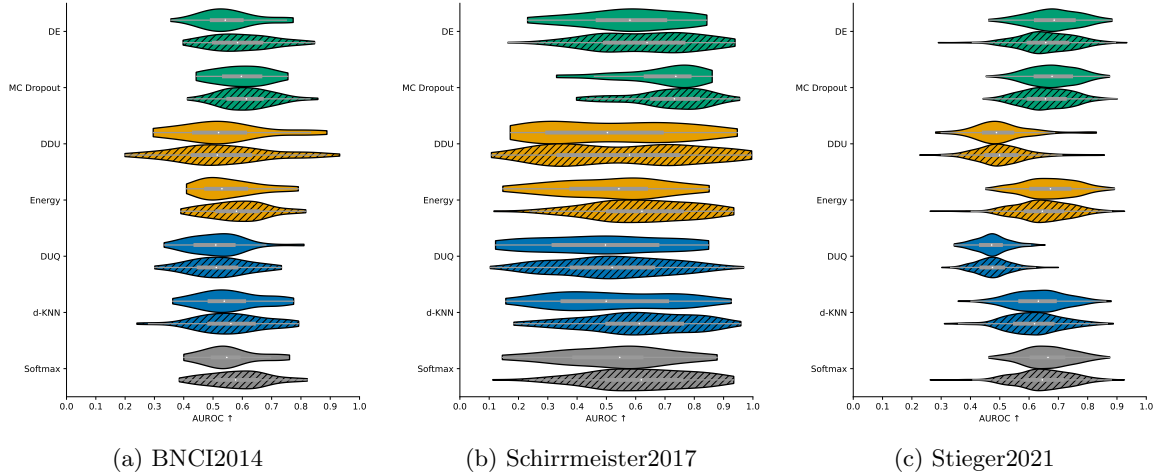


Figure B1: The difference between OOD detection when a model is trained on three classes \square or two classes hatched . Colours indicate the following UQ categories: Bayesian, Density, Distance, Baseline.

Method	BNCI2014		Schirrmeister2017		Stieger2021	
	p	Effect Size	p	Effect Size	p	Effect Size
Deep Ensemble	0.070	1866	0.058	4769	$8.440 \cdot 10^{-4}$	76575
MC Dropout	0.466	1669	0.335	4419	$1.319 \cdot 10^{-3}$	77056
DDU	0.941	1550	0.192	4547	0.158	94683
Energy	0.102	1834	$7.250 \cdot 10^{-4}$	5327	$1.100 \cdot 10^{-3}$	76858
DUQ	0.756	1593	0.268	4473	0.388	92592
d-KNN	0.756	1593	$4.399 \cdot 10^{-3}$	5127	0.027	80866
Softmax	0.081	1854	$3.562 \cdot 10^{-3}$	5152	0.035	81245

Table B1: Comparison of p-values and effect sizes from a Mann-Whitney U test across the three datasets for different methods. Bonferroni corrected $\alpha = 2.381\text{e-}3$

C Statistical analysis

C.1 OOD detection method comparison

Table C1 contains a summary of the Linear Mixed Model fitted on the results of the LOCO experiment with softmax on the BNCI2014 dataset as the baseline. As seen in the Table, the UQ methods perform significantly better on the Stieger2021 dataset compared to the BNCI2014 dataset. There is no significant difference between BNCI2014 and Schirrneister2017. Furthermore, DDU and DUQ perform significantly worse on the Stieger2021 dataset, while MC dropout performs significantly better on the Schirrneister2017 dataset.

Term	Coef.	Std.Err.	z	$P > z $	[0.025	0.975]
Intercept	0.554	0.026	21.716	$1.462 \cdot 10^{-104}$	0.504	0.605
Method[T.DDU]	-0.027	0.024	-1.136	0.256	-0.074	0.020
Method[T.DUQ]	-0.041	0.024	-1.705	0.088	-0.088	0.006
Method[T.Deep Ensemble]	0.000	0.024	0.009	0.993	-0.047	0.047
Method[T.Energy]	0.003	0.024	0.121	0.904	-0.044	0.050
Method[T.d-KNN]	0.006	0.024	0.251	0.801	-0.041	0.053
Method[T.MC Dropout]	0.042	0.024	1.763	0.078	-0.005	0.089
Dataset[T.Schirrneister2017]	-0.027	0.032	-0.834	0.404	-0.091	0.037
Dataset[T.Stieger2021]	0.109	0.027	4.026	$5.669 \cdot 10^{-5}$	0.056	0.163
Method[T.DDU]:Dataset[T.Schirrneister2017]	0.018	0.031	0.575	0.565	-0.042	0.077
Method[T.DUQ]:Dataset[T.Schirrneister2017]	-0.001	0.031	-0.046	0.964	-0.061	0.058
Method[T.Deep Ensemble]:Dataset[T.Schirrneister2017]	0.048	0.031	1.571	0.116	-0.012	0.108
Method[T.Energy]:Dataset[T.Schirrneister2017]	-0.015	0.031	-0.483	0.629	-0.075	0.045
Method[T.d-KNN]:Dataset[T.Schirrneister2017]	-0.012	0.031	-0.388	0.698	-0.072	0.048
Method[T.MC Dropout]:Dataset[T.Schirrneister2017]	0.123	0.031	4.020	$5.816 \cdot 10^{-5}$	0.063	0.182
Method[T.DDU]:Dataset[T.Stieger2021]	-0.135	0.026	-5.281	$1.283 \cdot 10^{-7}$	-0.185	-0.085
Method[T.DUQ]:Dataset[T.Stieger2021]	-0.150	0.026	-5.875	$4.220 \cdot 10^{-9}$	-0.200	-0.100
Method[T.Deep Ensemble]:Dataset[T.Stieger2021]	0.019	0.026	0.747	0.455	-0.031	0.069
Method[T.Energy]:Dataset[T.Stieger2021]	0.005	0.026	0.211	0.833	-0.045	0.055
Method[T.d-KNN]:Dataset[T.Stieger2021]	-0.037	0.026	-1.445	0.148	-0.087	0.013
Method[T.MC Dropout]:Dataset[T.Stieger2021]	-0.027	0.026	-1.052	0.293	-0.077	0.023
Group Var	0.003	0.005				

Table C1: Mixed Linear Effects Model Results (Dependent Variable: AUROC)

C.2 Pairwise comparison

Table C2 compares the UQ methods aggregated over the datasets. Softmax outperforms all other methods, while DDU and DUQ perform relatively similarly but worse than all other methods.

Contrast	Estimate	SE	z	p	P_{adj}
DDU - DUQ	0.025	0.011	2.368	0.0179	0.1073
DDU - Deep Ensemble	-0.089	0.011	-8.408	$4.164 \cdot 10^{-17}$	$6.662 \cdot 10^{-16}$
DDU - Energy	-0.066	0.011	-6.255	$3.987 \cdot 10^{-10}$	$3.987 \cdot 10^{-9}$
DDU - d-KNN	-0.056	0.011	-5.309	$1.103 \cdot 10^{-7}$	$9.924 \cdot 10^{-7}$
DDU - MC Dropout	-0.141	0.011	-13.296	$2.443 \cdot 10^{-40}$	$4.887 \cdot 10^{-39}$
DDU - Softmax	-0.066	0.011	-6.275	$3.503 \cdot 10^{-10}$	$3.854 \cdot 10^{-9}$
DUQ - Deep Ensemble	-0.114	0.011	-10.776	$4.460 \cdot 10^{-27}$	$8.474 \cdot 10^{-26}$
DUQ - Energy	-0.091	0.011	-8.623	$6.550 \cdot 10^{-18}$	$1.114 \cdot 10^{-16}$
DUQ - d-KNN	-0.081	0.011	-7.677	$1.630 \cdot 10^{-14}$	$2.282 \cdot 10^{-13}$
DUQ - MC Dropout	-0.166	0.011	-15.664	$2.669 \cdot 10^{-55}$	$5.604 \cdot 10^{-54}$
DUQ - Softmax	-0.091	0.011	-8.643	$5.491 \cdot 10^{-18}$	$9.884 \cdot 10^{-17}$
Deep Ensemble - Energy	0.023	0.011	2.154	0.0313	0.1563
Deep Ensemble - d-KNN	0.033	0.011	3.099	0.00194	0.0136
Deep Ensemble - MC Dropout	-0.052	0.011	-4.888	$1.020 \cdot 10^{-6}$	$8.160 \cdot 10^{-6}$
Deep Ensemble - Softmax	0.023	0.011	2.134	0.0329	0.1563
Energy - d-KNN	0.010	0.011	0.946	0.3444	1.000
Energy - MC Dropout	-0.074	0.011	-7.041	$1.903 \cdot 10^{-12}$	$2.474 \cdot 10^{-11}$
Energy - Softmax	-0.000	0.011	-0.020	0.9839	1.000
d-KNN - MC Dropout	-0.084	0.011	-7.987	$1.382 \cdot 10^{-15}$	$2.074 \cdot 10^{-14}$
d-KNN - Softmax	-0.010	0.011	-0.966	0.3342	1.000
MC Dropout - Softmax	0.074	0.011	7.021	$2.199 \cdot 10^{-12}$	$2.639 \cdot 10^{-11}$

Table C2: Pairwise contrast estimates with standard errors, z-scores, and adjusted p-values.

D Hyperparameters

Table D1 shows the hyperparameters used in the experiments for d-KNN and DUQ. Table D2 shows the search space in which the hyperparameters were found using the Optuna framework [1].

Class	k	Gamma (γ)	Centroid size	Penalty
<i>BNCI2014</i>				
Left hand	1	0.999	64	1.55×10^{-3}
Right hand	2	0.995	128	1.20×10^{-4}
Feet	12	0.913	64	1.19×10^{-5}
Tongue	106	0.995	128	1.20×10^{-4}
<i>BNCI2014 inversion</i>				
Left hand + Right hand	92	0.998	64	3.78×10^{-5}
Left hand + Feet	2	0.989	32	1.33×10^{-4}
Left hand + Tongue	5	0.989	32	1.33×10^{-4}
Right hand + Left hand	92	0.989	32	1.33×10^{-4}
Right hand + Feet	87	0.985	32	5.67×10^{-4}
Right hand + Tongue	5	0.913	64	1.19×10^{-5}
Feet + Left hand	48	0.999	64	1.55×10^{-3}
Feet + Right hand	7	0.913	64	1.19×10^{-5}
Feet + Tongue	77	0.979	128	3.77×10^{-3}
Tongue + Left hand	92	0.995	128	1.20×10^{-4}
Tongue + Right hand	92	0.998	64	3.78×10^{-5}
Tongue + Feet	92	0.959	256	3.73×10^{-2}
<i>Schürmeister2017</i>				
Right hand	18	0.989	32	1.33×10^{-4}
Left hand	4	0.989	32	1.33×10^{-4}
Rest	85	0.959	256	3.73×10^{-2}
Feet	62	0.998	64	3.78×10^{-5}
<i>Schürmeister2017 inversion</i>				
Right hand + Left hand	50	0.999	64	1.55×10^{-3}
Right hand + Rest	7	0.998	64	3.78×10^{-5}
Right hand + Feet	1	0.997	128	2.47×10^{-4}
Left hand + Right hand	71	0.999	64	1.55×10^{-3}
Left hand + Rest	1	0.989	32	1.33×10^{-4}
Left hand + Feet	1	0.998	64	3.78×10^{-5}
Rest + Right hand	45	0.995	128	1.20×10^{-4}
Rest + Left hand	71	0.975	32	2.09×10^{-3}
Rest + Feet	40	0.913	64	1.19×10^{-5}
Feet + Right hand	3	0.998	64	3.78×10^{-5}
Feet + Left hand	54	0.998	64	3.78×10^{-5}
Feet + Rest	84	0.995	128	1.20×10^{-4}
<i>Stieger2021</i>				
Right hand	9	0.902	256	5.67×10^{-4}
Left hand	43	0.989	64	1.42×10^{-4}
Both hands	2	0.995	32	1.11×10^{-2}
Rest	303	0.989	32	1.33×10^{-4}
<i>Stieger2021 inversion</i>				
Right hand + Left hand	46	0.970	32	2.14×10^{-2}
Right hand + Both hands	183	0.970	32	1.51×10^{-3}
Right hand + Rest	4	0.985	128	2.90×10^{-3}
Left hand + Right hand	34	0.984	128	3.28×10^{-4}
Left hand + Both hands	3	0.998	64	3.78×10^{-5}
Left hand + Rest	44	0.950	128	2.26×10^{-4}
Both hands + Right hand	1	0.986	128	2.65×10^{-4}
Both hands + Left hand	11	0.983	128	1.19×10^{-2}
Both hands + Rest	97	0.905	256	5.14×10^{-3}
Rest + Right hand	274	0.996	32	3.43×10^{-3}
Rest + Left hand	27	0.941	32	2.02×10^{-3}
Rest + Both hands	145	0.938	128	2.99×10^{-2}

Table D1: Hyperparameters for d-KNN (k) and DUQ (γ , centroid size, penalty) across all datasets. $\gamma = 1 - \text{one_minus_gamma}$. Penalty refers to the magnitude of the gradient penalty during training.

Hyperparameter	Search space	Scale
$1 - \gamma$	$[10^{-3}, 10^{-1}]$	Log-uniform
γ	$1 - (1 - \gamma)$	Derived
Centroid size	$\{32, 64, 128, 256\}$	Categorical
penalty	$[10^{-5}, 5 \times 10^{-2}]$	Log-uniform

Table D2: Hyperparameter search space used during optimization of the DUQ model.